Flux pinning properties of Yb substituted (Bi,Pb)-2212 superconductor

A. Biju [a], P.M. Sarun [a], R.P. Aloysius [b], U. Syamaprasad [a],*

[a] *Regional Research Laboratory (CSIR), Trivandrum 695019, India*
[b] *National Physical Laboratory (CSIR), New Delhi 110012, India*

Abstract

A systematic study on phase evolution, bulk density, resistivity, T_C, J_C, and J_C–B characteristics of pure and Yb substituted (Bi,Pb)-2212 samples at different cationic sites (Bi, Ca, Sr) has been carried out. The results show that there is a substantial improvement in the overall superconducting properties, particularly the T_C, J_C, and J_C–B characteristics of the Yb substituted samples. Further, it is observed that there is a significant shift in the peak value of the bulk pinning force density F_{pmax} towards higher magnetic fields when Yb is substituted at different cationic sites, indicative of the enhanced flux pinning strength in these samples. All the substituted samples show almost identical microstructure, but are distinctly different from pure (Bi,Pb)-2212. The natural layered growth mechanism of (Bi,Pb)-2212 is disrupted by grain growth, and coarsening in random directions. The substituted Yb atoms enter into the corresponding sites in (Bi,Pb)-2212, which create inhomogeneities in the crystal structure, decrease the hole concentration, and may produce point like defects. These defects act as the pinning centers. There is also the possibility of formation of nanoscale secondary phases, which can act as pinning centers.
© 2007 Elsevier B.V. All rights reserved.

PACS: 74.72.Hs; 74.25.Qt

Keywords: Superconductor; Solid state reactions; Electrical transport; Flux pinning and creep

1. Introduction

Even though $Bi_2Sr_2Ca_1Cu_2O_x$ (Bi-2212) superconductor has a higher transition temperature ($\sim$80 K), its effective use in magnet application is limited below 20 K because of its high electromagnetic anisotropy, short coherence length, and large penetration depth, which causes poor flux pinning properties at higher temperature. Extensive research work has been done to improve the superconducting and flux pinning properties of this system. It has been found that low angle grain boundaries, stacking faults, twin boundaries, impurity phases, precipitates, secondary phases, growth dislocation, point defects, oxygen vacancies, structural nonuniformities, and other objects of different dimensionality can act as pinning centers [1–17]. The doping of impurities with size of the order of the coherence length or creation of nanosize defects in the system by adjusting the processing condition can create effective pinning centers.

For instance increase in flux pinning strength was observed for Bi-2212 with nanosize MgO powders, whiskers, submicron precipitates of $SrZrO_3$, $SrSnO_3$, $CaCuO_3$ [9–13]. The impurities chosen for flux pinning should not deteriorate the superconducting properties, and its doping percentage should be critically adjusted. Even though in high T_C cuprates, the CuO_2 plane is believed to be responsible for the superconductivity. The doping at the Cu site in Bi-2212 is generally found to suppress the superconductivity [18,19]. But partial substitution of Pb for Bi in Bi-2212 reduces the anisotropy, improves structural modulation, and enhances irreversibility field [8]. Studies show that addition or substitution of rare earths in Bi-2212 enhances its superconducting properties such as J_C, and T_C. These substitution studies using rare earths on Ca, and Sr sites of (Bi,Pb)-2212 show that in the case of most of the rare earths the T_C, and J_C become maximum when the doping amount is between 0.2 and 0.3 in the stoichiometric level, irrespective of the site it is substituted [20–27].

In this work, we have prepared (Bi,Pb)-2212 samples by substituting the rare earth Yb at different cationic sites, viz. Bi, Ca, and Sr. We choose the doping amount of Yb as 0.25 in the sto-
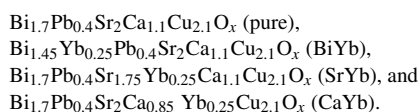
* Corresponding author. Tel.: +91 4712515373; fax: +91 4712491712.
E-mail address: syam@csrrltrd.ren.nic.in (U. Syamaprasad).

ichiometric level because for Yb the maximum T_C and J_C have been obtained in this range [22–24]. We show that Yb substitution at these cationic sites in (Bi,Pb)-2212 leads to significant improvement in the flux pinning strength of the samples along with increase of T_C and J_C. Most of the reported studies on the flux pinning have been conducted by estimating the magnetic J_C by dc magnetisation measurement. A meaningful measurement from application side is the measurement of transport J_C in presence of an applied magnetic field and we follow this in this work.

2. Experimental

Four set of (Bi,Pb)-2212 superconductor precursors (one pure and three Yb substituted) were prepared in the stoichiometric ratios:

$Bi_{1.7}Pb_{0.4}Sr_2Ca_{1.1}Cu_{2.1}O_x$ (pure),
$Bi_{1.45}Yb_{0.25}Pb_{0.4}Sr_2Ca_{1.1}Cu_{2.1}O_x$ (BiYb),
$Bi_{1.7}Pb_{0.4}Sr_{1.75}Yb_{0.25}Ca_{1.1}Cu_{2.1}O_x$ (SrYb), and
$Bi_{1.7}Pb_{0.4}Sr_2Ca_{0.85}Yb_{0.25}Cu_{2.1}O_x$ (CaYb).

All these samples were prepared by solid state synthesis route using high purity chemicals Bi_2O_3, PbO, $SrCO_3$, $CaCO_3$ CuO, and Yb_2O_3 (Aldrich, >99.9%). Stoichiometric amounts of the ingredients were weighed using an electronic balance (Mettler AE 240), thoroughly mixed and ground using an agate mortar and pestle, and then subjected to a three stage calcination process in air at temperatures 800 °C/15 h, 820 °C/30 h, and 840 °C/60 h, with a heating rate of 3 °C/min. Intermediate wet grinding was done between each stages of calcination. After calcination the samples were pelletized using a cylindrical die of 12 mm diameter under a force of 60 kN. The pellets were then heat treated at 848 °C for 100 h (50 + 50) in two stages with one intermediate re-pressing under a force of 60 kN.

Phase analysis of the samples was done using X-ray diffraction (XRD) (Philips *X'pert Pro*) employing X'celerator and monochromater at the diffracted beam side. Phase identification was performed using *X'Pert High score* software in support with ICDD-PDF 2 database. The densities of the pellets before and after the two stages of sintering were calculated by measuring the mass and dimensions of the pellets. Transport J_C measurements were done at 64 K using the four probe method with the standard criterion of 1 μV/cm. The transport current dependence on magnetic field (J_C–B) was studied using a homemade set-up with field ranging from 0–1 T. Rectangular samples of dimensions about 12 mm × 3 mm × 1 mm cut from round pellets were used for the J_C–B measurements. A Lakeshore temperature controller (Model: 340) was used to accurately monitor the temperature. The critical temperature of the samples also was measured using four probe method by varying the temperature from 64 K using a bath cryostat. Microstructural examinations of the samples were done using scanning electron microscopy (SEM) (JEOL JSM 5000LV). Elemental analyses of the samples were done using energy dispersive X-ray analysis (EDX) attached to the SEM.

3. Results and discussion

Fig. 1 shows the XRD patterns of the samples after the calcination at 820 °C/30 h. All samples contains (Bi,Pb)-2212 as the major phase along with Bi-2201, and Ca_2PbO_4 as secondary phases. A careful analysis of the patterns shows that the secondary phases are lesser in the Yb substituted samples compared to the pure one. This indicates that Yb substitution favours the formation of (Bi,Pb)-2212 irrespective of the site it is substituted. Along with (Bi,Pb)-2212, Bi-2201, and Ca_2PbO_4 phases are also present in all the samples, at this stage. XRD patterns of the samples after the last stage heat treatment are shown in Fig. 2. In these patterns, all the peaks are of (Bi,Pb)-2212. Thus, phase
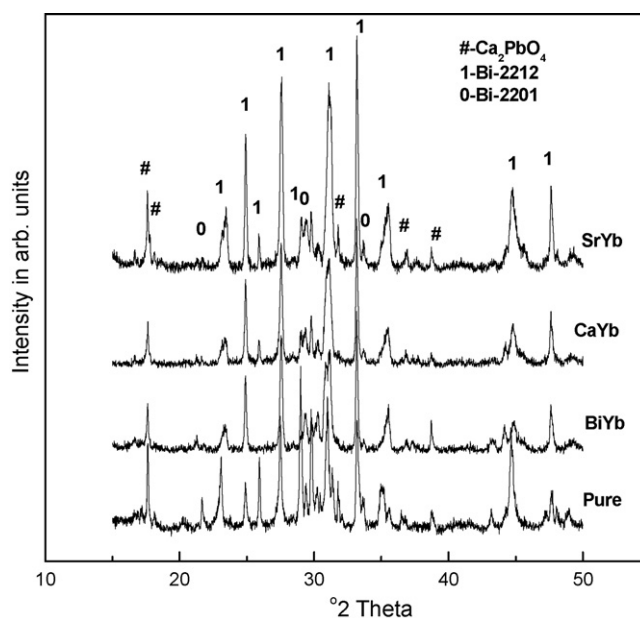

Fig. 1. XRD patterns of the samples after 820 °C/30 h.

pure (Bi,Pb)-2212 is obtained by the last stage of heat treatment at 845 °C for 100 h. No secondary phase containing Yb or other cations could be detected from XRD analysis. This indicates that Yb enters into the (Bi,Pb)-2212 structure in all the three cationic substitutions. The variations of c-axis parameter with substitution at different sites are shown in Table 1. The lattice parameter calculations were based on orthorhombic symmetry assumed for (Bi,Pb)-2212. It is observed that the substitution of rare earths in Bi-2212 causes contraction of c-axis length as reported in some of the earlier works [24–27]. This contraction in c-axis length also shows that the doped atoms enter into the crystal structure. The reason for the decrease in c-axis is due to
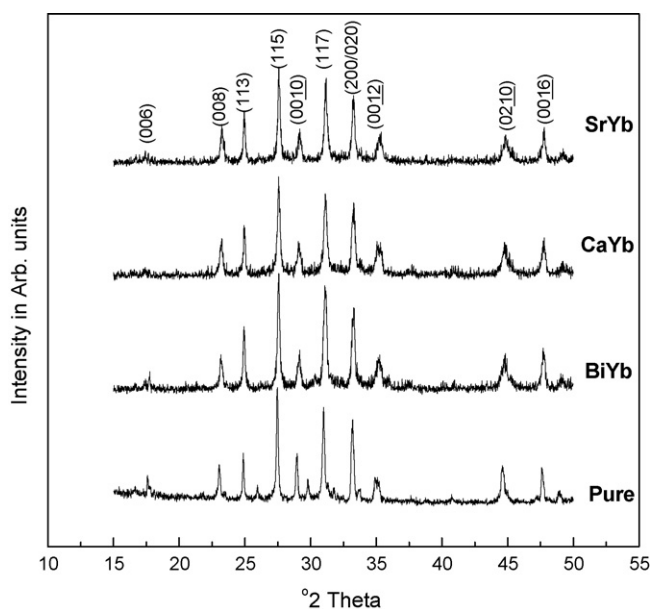

Fig. 2. XRD patterns of the samples after last stage heat treatment(all the peaks are of (Bi,Pb)-2212).

Table 1
Sintered density, T_C, ΔT_C, J_C, normal state resistivity, and c-axis length of pure, and Yb substituted (Bi,Pb)-2212 samples

Sample	Final sintered density(g cm^{-3})	T_C (K)	ΔT_C (K)	J_C at 64 K (A/cm^2)	Normal state resistivity at 300 K ($\mu\Omega$ m)	c-axis length (Å)
Pure	5.506	80.3	1.08	100.5	11	30.800
BiYb	5.175	97.5	9.14	655	33.2	30.652
CaYb	5.566	96.5	9.8	1435	46.2	30.647
SrYb	5.516	95	8.7	721	26	30.590

the increase in oxygen content in the system because of the substitution of higher valence cations. The replacement of Ca^{2+} or Sr^{2+} ions by Yb^{3+} ions causes an increase in the oxygen content. This excess oxygen is taken up by the Bi–O double planes, causing a tighter binding, which reduces the c-axis length [25]. In the case of Bi-site substitution, though the valency is the same, some of the substituted Yb^{3+} ions are likely to enter into Ca or Sr sites, and cause an increase in oxygen content. The reduction of c-axis is found to be higher when the substitution is made in the Sr-site. This indicates that even if the amount of initial stoichiometry of Yb is kept the same for different cations, more atoms of Yb go to the Sr-site after the reaction due to the higher ionic radius of Sr^{2+} (1.12 Å) compared to Ca^{2+} (0.99 Å) and Bi^{3+}(0.96 Å).

Fig. 3 shows the variation of density of the samples at different stages of processing. The density values as percentages of theoretical density of (Bi,Pb)-2212 (6.6 g cm^{-3}) are shown on the right axis of the figure. The sintered densities of all the samples are less than the corresponding density prior to heat treatment (green density). It is usually referred to as 'retrograde densification', and it is a characteristic property of BSCCO system. The densities of the samples are found to vary with Yb substitution at different cationic sites. Samples SrYb and CaYb show an increase in density while BiYb shows a reduction compared to the pure sample.
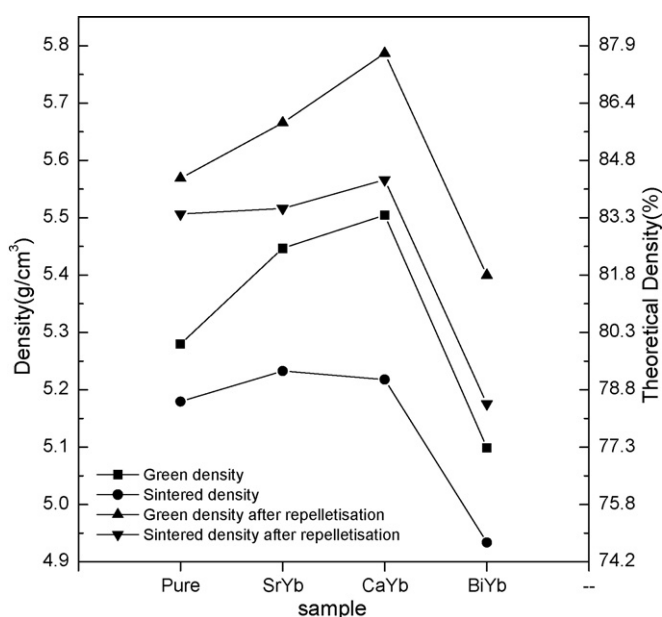

Fig. 3. Density variations of the samples with substitution at different cationic sites.

The SEM pictures of fractured pellets taken in the back scattered mode are displayed in Fig. 4. The grain morphology of the samples shows a clear, and distinct variation in pure, and doped samples. For pure (Bi,Pb)-2212, clear, and flaky grains with layered growth are obtained. But in the case of all doped samples the grain size decreases, the flaky nature of the grains changes, and the edges of the grains become rounded. BiYb samples show relatively smaller grains as compared with the other doped samples. Also in the doped samples, dark round shaped grains are found scattered in the main matrix as a secondary phase, but the presence of such a phase was not detected in the XRD patterns.

Fig. 5 shows the EDX spectra of a relatively large area of the (Bi,Pb)-2212 grains of pure and doped samples along with that of the secondary phase in BiYb sample. Quantitative values obtained from EDX analysis of the cations in (Bi,Pb)-2212 grains Fig. 5(a–d) are given in Table 2 which show that the grains of all the three doped samples contain Yb with corresponding reduction in Bi/Sr/Ca. This is clear evidence that most of the Yb atoms enter into the corresponding sites where these are intended to substitute. The spectrum of secondary phase in BiYb sample Fig 5(e) contains mainly Sr and Ca, and doesn't have any Yb. This shows that when Yb is substituted in the Bi site, few Yb atoms enter into the Sr and Ca sites, and the replaced Sr and Ca react with Cu and (Bi,Pb) forming the secondary phase.

Fig. 6 shows the temperature dependence of resistivity of the samples. All samples show a metallic behavior in the normal state with a metal-superconductor transition. Transition temperatures of all the Yb substituted samples show a significant increase as compared to the pure sample (Table 1). For example, the T_C of BiYb increases to 97.5 K from 80.5 K measured for the pure sample. The ΔT_C ($T_{C\text{-onset}} - T_{C\text{-zero}}$), and the normal state resistance (Table 1) of the doped samples are higher as compared with the pure sample. This is because the doped samples contain higher levels of impurities, and lattice disorder. The critical current densities of the samples are also considerably enhanced by Yb substitution. For example, when the pure sample shows a J_C of 100.5 A cm^{-2}, CaYb sample shows a J_C of 1435 A cm^{-2}, which is about 14 times higher than that of the pure sample prepared in similar conditions. J_C of different samples are shown in Table 1.

The field dependence of the normalized J_C [$J_C(B)/J_C(0)$] is shown in Fig. 7. The corresponding J_C–B plots are given in the inset of the figure. The J_C–B characteristics of Yb substituted samples are found to be much better than that of the pure sample. That is, the deterioration of J_C due to the magnetic field is significantly reduced as a result of the substitution. This shows that substitution of Yb at cationic sites enhances the flux pinning properties of (Bi,Pb)-2212. Using the volume pinning force den-
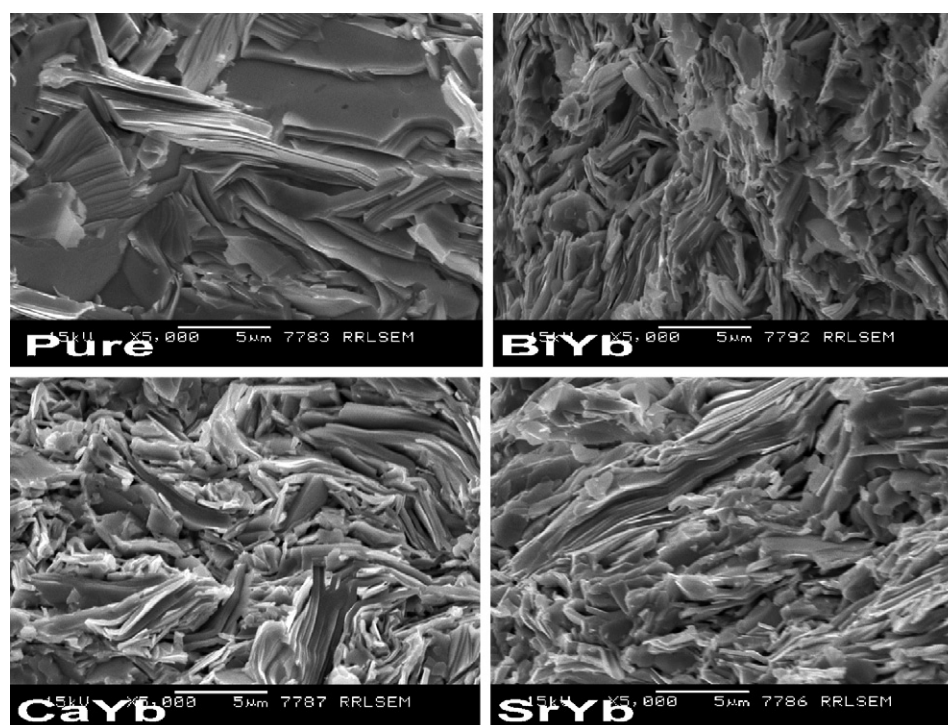
Fig. 4. SEM micrographs of the samples taken in the back scattered mode.

sity, $F_p = J_C \times B$, one can investigate the flux pinning strength of the system [28–31]. The normalized volume pinning force density (F_p/F_{pmax}) calculated from the data of Fig. 7 as a function of the applied field is plotted in Fig. 8. It is seen that substitution of Yb shifts the peak positions of F_p/F_{pmax} towards higher fields. For example, for the pure sample the peak value of F_p/F_{pmax} appears at around 0.08 T, whereas for BiYb and CaYb the peak values appear beyond 0.7 T. This indicates that the irreversibility line (IL) of Yb substituted samples gets shifted towards higher fields. This confirms that the flux pinning strength of (Bi,Pb)-2212 increases significantly when Yb is substituted for cationic sites. It is also clear from Fig. 8 that the flux pinning strength is maximum when the substitutions are in Ca or Bi sites as compared with Sr site. The J_C–B plots also show that flux pinning is better for these samples.

For polycrystalline samples different pinning mechanisms exist which are simultaneously active. In the case of high T_C-materials, one can assume that core pinning is dominant due to large Ginzberg-Landau parameters (κ) of these materials. This leaves two different sources of pinning, either by nonsuperconducting particles embedded in the superconducting matrix leading to a scattering of mean free path (δl pinning) or pinning provided by spatial variations of the κ values associated with transition temperature T_C (δT_C or $\Delta \kappa$ pinning). Recent studies [32] on single crystals show that Bi–Sr nonstoichiometry affects the T_C of Bi-based superconductors. Pure Bi-2212 is highly nonstoichiometric. Substitution of rare earths in the cationic sites can change the Bi–Sr nonstoichiometry. Increase in the flux pinning properties, and shifting of IL towards higher magnetic field suggest that the inhomogeneities can affect flux pinning properties of the samples also. The introduction of Yb^{3+} ions at the cationic sites creates change in chemical as well as electronic inhomogeneities, which may induce point like defects in the crystals. These defects can act as flux pinning

Table 2
Quantitative EDX results of cation stoichiometry of pure, and Yb doped(Bi,Pb)-2212 grains

Sample	Stoichiometry	(Bi,Pb)	Sr	Ca	Cu	Yb
Pure	Initial	2.10	2.00	1.10	2.10	0.00
	From EDX	2.09	2.11	1.0	2.70	0.00
BiYb	Initial	1.85	2.00	1.10	2.10	0.25
	From EDX	1.89	2.13	0.90	2.94	0.38
SrYb	Initial	2.10	1.75	1.10	2.10	0.25
	From EDX	1.90	1.74	1.00	2.65	0.29
CaYb	Initial	2.10	2.00	0.85	2.10	0.25
	From EDX	2.03	2.24	0.85	2.72	0.38

Fig. 6. Resistivity-temperature plots of the samples.
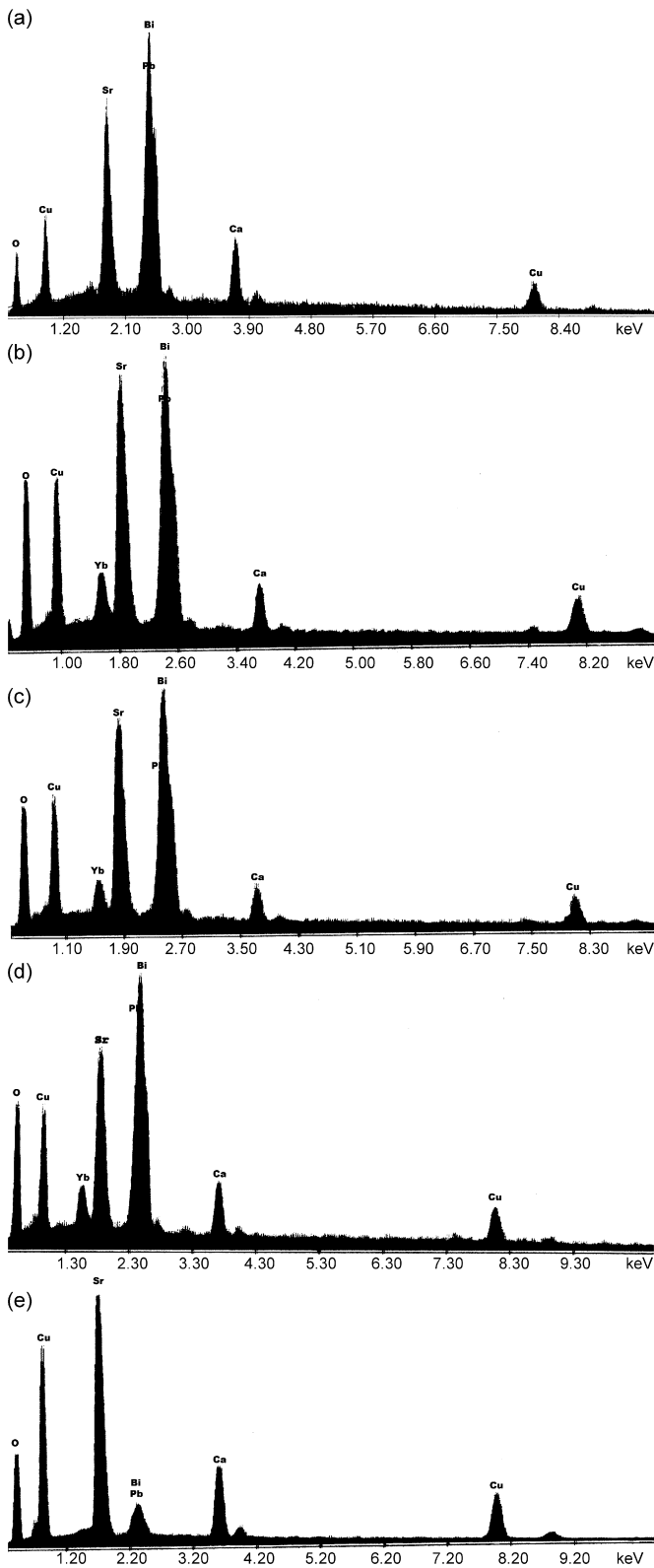

Fig. 5. EDX spectra of (Bi,Pb)-2212 grains of (a) Pure (b) BiYb (c) CaYb (d)SrYb, and (e) the secondary phase in BiYb.

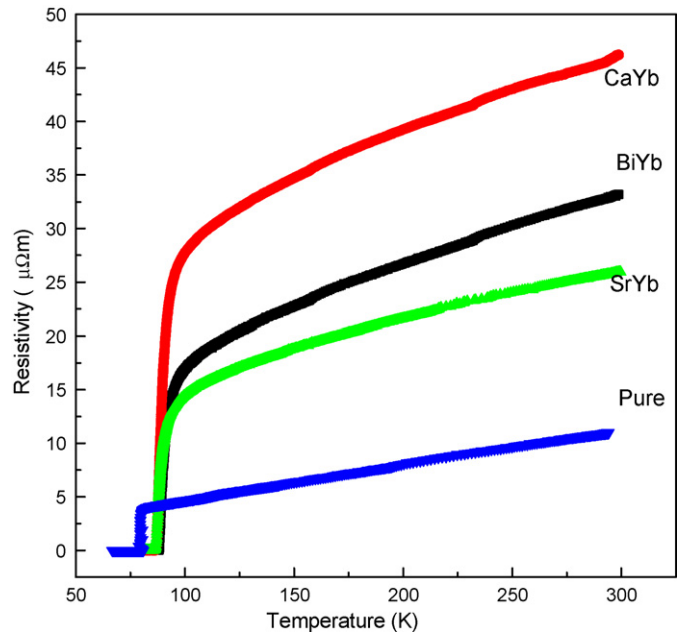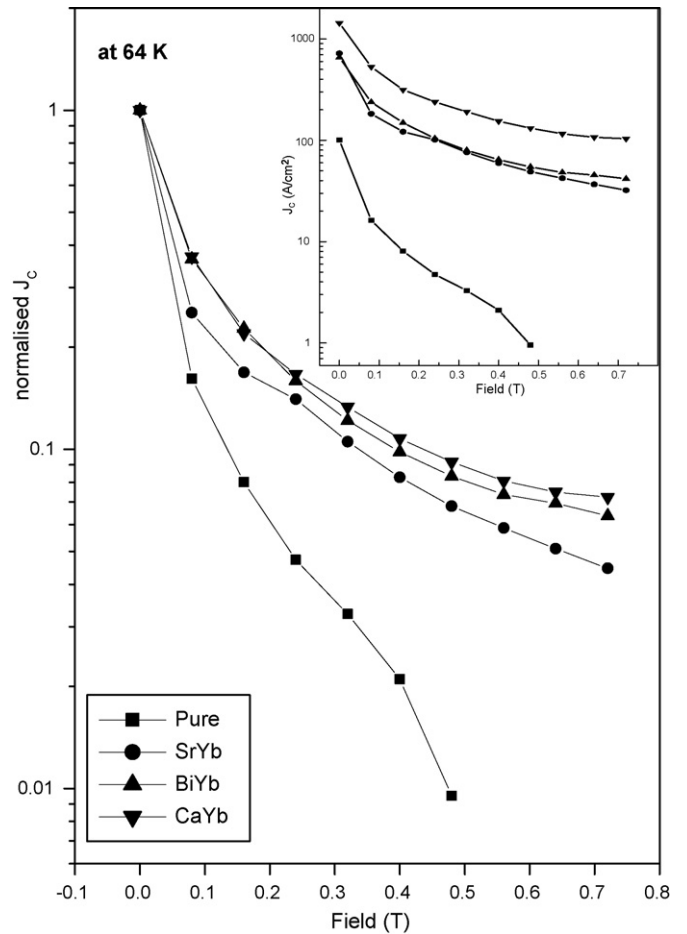Fig. 7. Variation of the normalized J_C as a function of the applied field (inset: J_C–B characteristics).
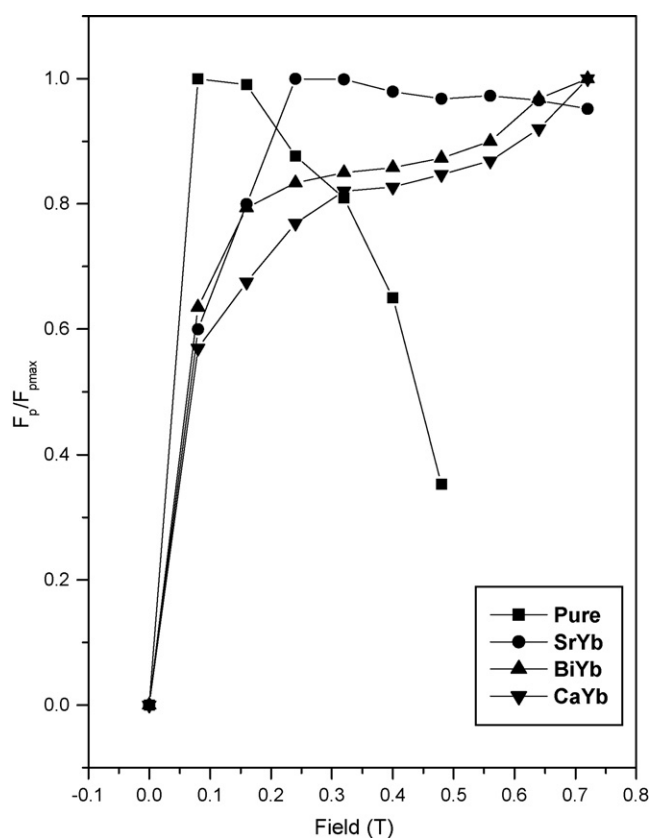
Fig. 8. Variation of the normalized pinning force density as a function of applied field.

centers. There is also a possibility of formation of nanoscale secondary phases scattered in the samples due to the substitution of Yb, which can act as flux pinning centers. The enhancement of T_C and J_C can also be related to inhomogeneities, and the decrease in the charge carrier (holes) concentration due to the replacement of divalent cations by trivalent Yb ions. Even in the case of Bi site substitution few Yb atoms goes to Sr and Ca sites, which changes the charge carrier concentration. This is clear from the EDX of the secondary phase of BiYb sample [Fig. 5(e)].

4. Conclusion

Yb substitution at different cationic sites such as Bi, Sr, Ca in (Bi,Pb)-2212 enhances T_C, J_C, and flux pinning strength of the system if the amount of substitution is in the optimum level ($x = 0.25$), and these properties depend on the cationic site in which Yb is substituted. The J_C–B characteristics of the substituted samples show substantial improvement over the undoped sample. The peak value of the bulk pinning force density (F_{pmax}) also gets shifted towards higher fields for the doped samples indicative of a shift of IL towards higher fields. The enhancements of the superconducting and flux pinning properties are discussed based on the changes in the chemical as well as electronic inhomogeneities in the samples due to Yb substitution.

References

[1] H.L. Su, P. Majenski, F. Aldinger, Physica C 249 (1995) 241–246.
[2] P. Majenski, S. Elschner, F. Aldinger, Physica C 249 (1995) 234–240.
[3] P. Majenski, S. Elschner, B. Hettich, C. Lang, S. Kaesche, F. Aldinger, Supercond. Sci. Technol. 7 (1994) 514–517.
[4] T.W. Li, R.J. Drost, P.H. Ker, C. Tracholt, H.W. Zandbergen, N.T. Hien, A.A. Menovsky, J.J.M. Franse, Physica C 274 (1997) 197–203.
[5] A. Amira, M.F. Mosbah, P. Molinie, A. Leblanc, Solid State Sci. 7 (2005) 53–57.
[6] S. Wu, J. Schwartz, G.W. Raban Jr, Physica C 246 (1995) 297–308.
[7] K.K. Uprety, J. Howat, X.L. Wang, M. Ionescu, H.K. Liu, S.X. Doe, Supercond. Sci. Technol. 14 (2001) 479–485.
[8] I. Chong, M. Hiroi, J. Izumi, Y. Shimoyema, Y. Nakayama, K. Kishio, T. Terashima, Y Bando, Y Takam, Science 276 (1997) 770–773.
[9] W. Wei, J. Schwartz, K.C. Goretta, U. Balachandran, A. Bhargava, Physica C 298 (1998) 279–288.
[10] P. Yang, C.M. Lieber, Science 273 (1996) 1836–1840.
[11] P.E. Kazin, M. Jansen, A. Larrea, G.F de la Fuente, Y.D Tretyakov, Physica C 253 (1995) 391–400.
[12] P.E. Kazin, A.S. Karpov, Y.D. Tretyakov, M. Janson, Solid State Sci. 3 (2001) 285–290.
[13] T. Umemura, A. Nozaki, K. Egama, F. Uchikawa, J. Sato, J. Appl. Phys. 31 (1992) 2698–2703.
[14] P. Sen, S.K. Bandyopadhyay, P.M.G. Nambissan, P. Barat, P. Mukherjee, Solid State Sci. 4 (2002) 783–786.
[15] M. Mironova, D.F. Lee, K. Salama, Physica C 211 (1993) 188–204.
[16] L. Civale, A.D. Marwick, I.V. Wheeler, M.A. Kirk, W.L. Carter, G.N. Riley Jr., A.P Malozemoff, Physica C 208 (1993) 137–142.
[17] P. Kummeth, H.-W. Neumuller, G. Ries, M. Krans, S. Klamiinzer, G. Seeman-Ischenko, J. Alloys Compd. 195 (1993) 403–406.
[18] J.M. Tarascon, P. Barboux, P.F. Miceli, L.H. Greene, G.W. Hull, M. Eibshutz, S.A. Sunshine, Phys. Rev. B: Condens. Matter 37 (1998) 7458–7469.
[19] B. Vom Hedt, W. Liieck, K. Westerholt, H. Back, Phys. Rev. B: Condens. Matter 49 (1994) 9898–9905.
[20] R. Somasundaram, R. Vijayaraghavan, R. Nagarajan, R. Seshadri, A.M. Umarji, C.N.R. Rao, Appl. Phys. Lett. 56 (1990) 487–489.
[21] R. Yoshizaki, J. Fujikami, M. Akamatsu, H. Ikda, Supercond. Sci. Technol. 4 (1991) S421-S423.
[22] T. Motohashi, Y. Nakayama, T. Fujita, K. Kitazawa, J. Shimayama, K. Kishio, Phys. Rev. B: Condens. Matter 59 (1999) 14080–14086.
[23] H. Fuji, Y. Hishinuma, H. Kitaguchi, H. Kumakura, K. Togano, Physica C 331 (2000) 79–84.
[24] H. Jin, J. Kotzler, Physica C 325 (1999) 153–158.
[25] C. Nguyen-van Huong, C. Hinnen, J.M. Siffre, J. Mater. Sci. 32 (1997) 1725–1731.
[26] A. Biju, R.P Aloysius, U. Syamaprasad, Supercond. Sci. Technol. 18 (2005) 1454–1459.
[27] R.P. Aloysius, P. Guruswamy, U. Syamaprasad, Supercond. Sci. Technol. 18 (2005) L23–L28.
[28] M.R. Koblischka, A.J.J. Van Dalen, T. Higuchi, S. Yoo, M. Murakami, Phy. Rev. B: Condens. Matter 58 (1998) 2863–2867.
[29] M.R. Koblischka, M. Murakami, Supercond. Sci. Technol. 13 (2000) 738–744.
[30] E.J. Karmer, J. Appl. Phys. 44 (1973) 1360–1370.
[31] D. Dew- Hughes, Philos. Mag. 30 (1974) 293.
[32] H. Eisaki, N. Kaneko, D. Feng, L. Feng, A. Damascelli, P.K. Mang, K.M. Shen, Z.X. Shen, M. Greven, Phys. Rev. B: Condens. Matter 69 (2004), 064512-1-8.